Click Here for Full Article

Feasibility of soil moisture estimation using passive distributed temperature sensing

S. C. Steele-Dunne,[1] M. M. Rutten,[1] D. M. Krzeminska,[1] M. Hausner,[2] S. W. Tyler,[2] J. Selker,[3] T. A. Bogaard,[1] and N. C. van de Giesen[1]

Received 7 June 2009; revised 25 September 2009; accepted 16 October 2009; published 30 March 2010.

[1] Through its role in the energy and water balances at the land surface, soil moisture is a key state variable in surface hydrology and land-atmosphere interactions. Point observations of soil moisture are easy to make using established methods such as time domain reflectometry and gravimetric sampling. However, monitoring large-scale variability with these techniques is logistically and economically infeasible. Here passive soil distributed temperature sensing (DTS) will be introduced as an experimental method of measuring soil moisture on the basis of DTS. Several fiber-optic cables in a vertical profile are used as thermal sensors, measuring propagation of temperature changes due to the diurnal cycle. Current technology allows these cables to be in excess of 10 km in length, and DTS equipment allows measurement of temperatures every 1 m. The passive soil DTS concept is based on the fact that soil moisture influences soil thermal properties. Therefore, observing temperature dynamics can yield information on changes in soil moisture content. Results from this preliminary study demonstrate that passive soil DTS can detect changes in thermal properties. Deriving soil moisture is complicated by the uncertainty and nonuniqueness in the relationship between thermal conductivity and soil moisture. A numerical simulation indicates that the accuracy could be improved if the depth of the cables was known with greater certainty.

Citation: Steele-Dunne, S. C., M. M. Rutten, D. M. Krzeminska, M. Hausner, S. W. Tyler, J. Selker, T. A. Bogaard, and N. C. van de Giesen (2010), Feasibility of soil moisture estimation using passive distributed temperature sensing, *Water Resour. Res.*, *46*, W03534, doi:10.1029/2009WR008272.

1. Introduction

[2] Because of its role in the water and energy balances at the land surface, soil moisture has been identified as a key state variable in surface hydrology and land-atmosphere interactions [*Entekhabi et al.*, 1996]. In the coming 5 years, the European Space Agency and the National Aeronautics and Space Administration will launch the first dedicated satellite missions (Soil Moisture and Ocean Salinity (SMOS) and Soil Moisture Active and Passive (SMAP)) to measure this critical state variable [*Anthes et al.*, 2007; *Kerr et al.*, 2001]. Data from these missions will be used to improve our understanding of the global energy and water budgets. For calibration and validation, a global network of independent in situ soil moisture measurements over varying soil and land cover types is essential. Point observations of soil moisture are relatively straightforward to make using established methods such as time domain reflectometry (TDR) and gravimetric sampling. TDR is a useful method for making continuous, long-term measurements as it is nondestructive, and sensors can be installed at the site of interest. However, monitoring large-scale variability with TDR would involve installing a vast and costly network of sensors.

[3] Here we propose using distributed temperature sensing (DTS) to obtain simultaneous measurements of soil moisture over large areas. By providing continuous, high-resolution observations over a large area, soil DTS could play an important role in supporting a modest network of traditional sensors. Soil moisture fields can maintain spatial patterns in time because of covariances between soil moisture and factors such as topography, soil texture, and vegetation [*Vachaud et al.*, 1985; *Mohanty and Skaggs*, 2001; *Jacobs et al.*, 2004; *Cosh et al.*, 2004]. Temporal and spatial stability concepts can be used to identify a single or a few representative sensor locations, observations which are similar to the field or pixel average. Alternatively, they can also be used to identify locations that are systematically biased with respect to the mean, thereby providing a measure of subfield or subpixel heterogeneity. Quantifying spatiotemporal stability requires an extensive initial network of sensors to measure soil moisture over a lengthy validation period. Soil DTS offers a relatively economical way to make continuous observations at thousands of locations within the watershed or footprint of interest. Furthermore, combining a few accurate, conventional sensors with the distributed observations from soil DTS to capture fine-scale variability in soil moisture would enhance the usefulness of large-scale remote sensing products.

[1]Water Resources Section, Faculty of Civil Engineering and Geosciences, Delft University of Technology, Delft, Netherlands.
[2]Department of Geological Sciences and Engineering, University of Nevada, Reno, Reno, Nevada, USA.
[3]Department of Biological and Ecological Engineering, Oregon State University, Corvallis, Oregon, USA.

Copyright 2010 by the American Geophysical Union.
0043-1397/10/2009WR008272

[4] The idea of observing temperature dynamics to infer soil moisture is far from new. *Idso et al.* [1975a, 1975b, 1976] explored the possibility of using the thermal inertia of the surface to infer soil moisture in the top few centimeters of the soil column. *Price* [1977] proposed an algorithm based on an "apparent thermal inertia," calculated from satellite observations of daily minimum and maximum temperature and surface reflectance, which might be used to estimate soil moisture from remote sensing. In addition to the challenges posed by thermal infrared remote sensing (notably, atmospheric attenuation and vegetation opacity), the thermal inertia approach also needed to account for the surface energy balance [e.g., *Rosema*, 1975; *Gurney and Camillo*, 1984] as well as the subsurface soil moisture lower boundary condition [*Van De Griend et al.*, 1985].

[5] The dependence of soil thermal properties on soil moisture has also been used to design in situ soil moisture probes. Most are based on the initial dual-probe heat pulse design of *Campbell et al.* [1991]. Many have been augmented with additional needles to allow for simultaneous measurement of water flow, solute, and heat transport properties [e.g., *Mori et al.*, 2003; *Mortensen et al.*, 2006]. Recent designs include a "button" heat pulse probe, in which a ring-shaped heating element and a central thermistor are embedded in a plastic disk [*Kamai et al.*, 2008]. This new design addresses the sensitivity of results from conventional heat pulse probes to needle spacing [*Kluitenberg et al.*, 1995; *Liu et al.*, 2008]. Nonetheless, these probes still measure soil moisture at a single location. The proposed methodology will use hundreds or thousands of temperature measurements over a large area to monitor soil moisture in a distributed fashion.

[6] Distributed temperature sensing is a flexible and powerful tool in environmental monitoring in which temperature changes are measured along a fiber-optic cable [e.g., *Selker et al.*, 2006]. When laser light is sent through fiber-optic cable, a small fraction of the energy undergoes inelastic (Raman and Brillouin) scattering whereby light is produced at frequencies higher (anti-Stokes signal) and lower (Stokes signal) than the transmitted laser light. The amplitude of the backscattered anti-Stokes signal is a function of the cable temperature and the intensity of illumination. The amplitude of the Stokes signal is a function of the intensity of illumination alone. Consequently, the ratio of the anti-Stokes and Stokes intensities provides a measure of the cable temperature [*Tyler et al.*, 2009]. The spatial resolution of commercially available DTS is typically 1 m for cables up to 10 km long. The precision of the temperature measurement depends on laser intensity, detector sensitivity, and integration time, but precision on the order of 0.1 K can be obtained using a 1 km cable with 1 m resolution and a 60 s integration time. *Selker et al.* [2006] demonstrated the potential usefulness of DTS in diverse hydrological investigations.

[7] Recently, Sayde et al. (Feasibility of soil moisture monitoring with fiber optics, submitted to *Water Resources Research*, 2009) demonstrated that soil moisture in a laboratory column in the range 0.05–0.41 $m^3\ m^{-3}$ could be measured with a precision of 0.046 $m^3\ m^{-3}$ using an active DTS approach. In active DTS, a heat pulse is applied to the soil, and the resultant temperature change in the fiber-optic cable is used to determine soil moisture. Alternatively, passive soil DTS measures the temperature response in buried cables to the diurnal radiation cycle. Because passive soil DTS avoids applying external energy to the soil column, the soil temperature and flux profiles are undisturbed and the natural state can be observed.

[8] Active DTS also poses logistical (and economical) challenges to its implementation in the field. The only power demand of passive soil DTS is that of the DTS unit and data recorder, while active DTS also requires a power source to heat one of the cables. Installing a passive soil DTS system involves plowing the fiber-optic cable into the ground. Active DTS requires electrical connections where current can be applied to heat the cable. The reduced power requirement and simpler installation render passive soil DTS a more flexible and inexpensive tool than active DTS.

[9] There are two potential roles for passive soil DTS.

[10] 1. If passive soil DTS alone can yield an adequate estimate of soil moisture, it could be used to monitor soil moisture over large scales for long time periods.

[11] 2. Passive and active soil DTS could be combined. Active soil DTS could be reserved for periods when the site is managed because a high-voltage subsurface installation requires supervision. Passive soil DTS could provide continuity between managed periods.

[12] In this study, results from a feasibility study are presented which demonstrate that passive soil DTS alone can yield information on surface soil moisture. From June to September 2008, fiber-optic cables were used to monitor temperature at two depths at a field site at Monster, Netherlands. Through its impact on thermal diffusivity, soil moisture influences heat transport between the cables. Here it is shown that solving for the optimum parameters of the heat diffusion equation can yield a time series of estimated soil moisture. The challenges associated with inferring soil moisture from temperature data, the lessons learned from this experiment, and a new strategy for using this technique in future field experiments are also discussed.

2. Methods

[13] The hypothesis of this research is that soil moisture can be determined from temperature data because of the dependence of soil thermal properties on soil moisture. First, the thermal diffusivity must be determined from the observed cable temperatures. Then, the soil moisture must be inferred from the thermal diffusivity.

2.1. Soil Thermal Properties From Cable Temperatures

[14] Heat transfer in a soil column can be described by the diffusion equation

$$\frac{\partial T}{\partial t} = D(\theta)\frac{\partial^2 T}{\partial z^2} = \frac{\kappa(\theta)}{C(\theta)}\frac{\partial^2 T}{\partial z^2}, \tag{1}$$

where T is temperature and D is the thermal diffusivity of the soil, the ratio of its thermal conductivity (κ) to its thermal capacity (C). These soil thermal properties are functions of soil moisture, so the objective of this feasibility study was to determine if soil temperature measurements at multiple levels are sufficient to infer soil thermal properties and hence soil moisture. Using an approach similar to that employed by *Béhaegel et al.* [2007], soil moisture was estimated by finding the diffusivity which gave the best fit between simulated and observed cable temperature.

[15] An implicit finite difference scheme was used to simulate heat diffusion in a soil column from the surface to

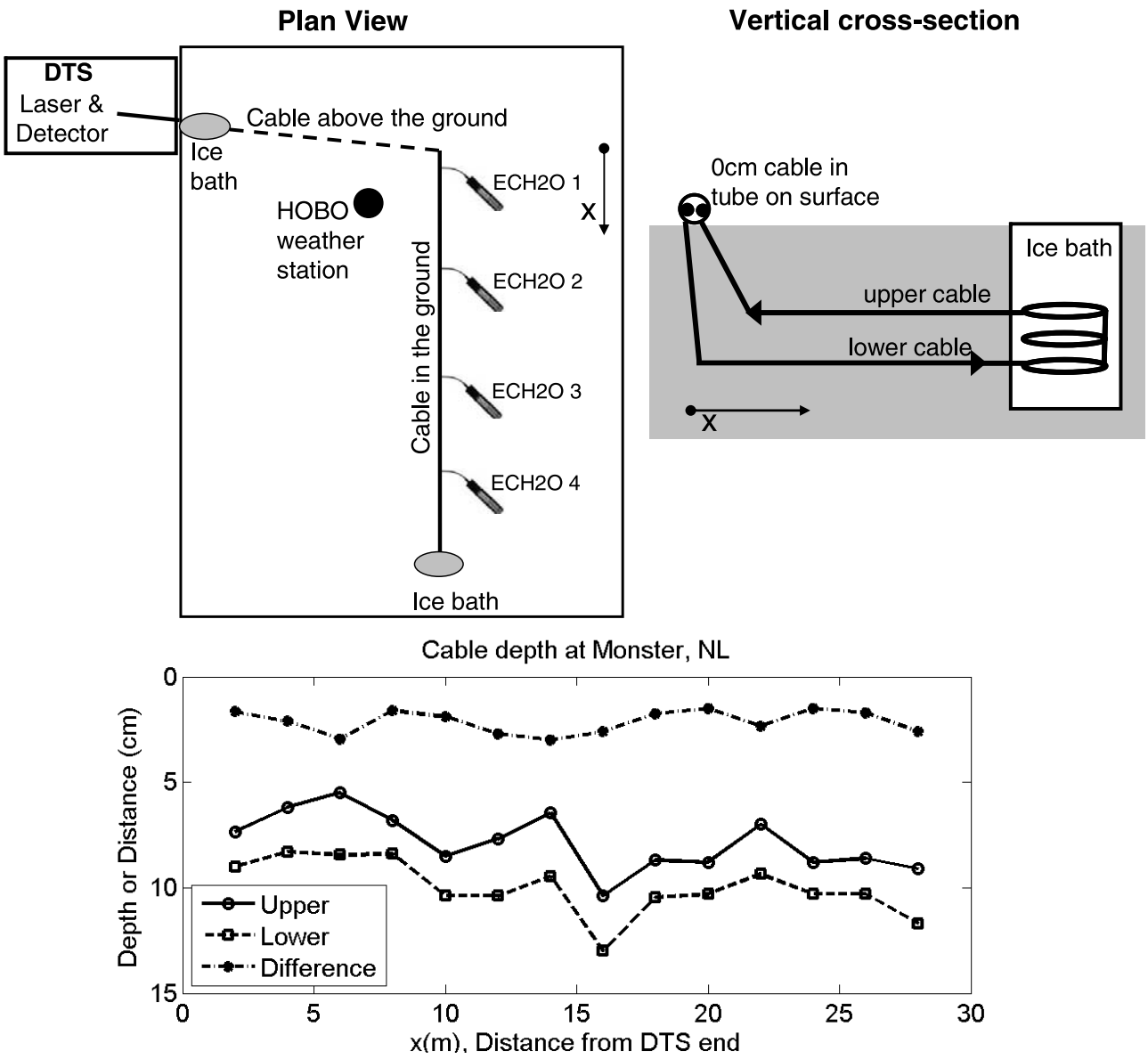

Figure 1. Experiment setup. (top) Plan view and vertical cross section of cable installation at Monster, Netherlands. (bottom) Measured cable depth as a function of distance from the DTS end (x = 2 m refers to the cable segment between 0 and 2 m).

the depth of the lower cable at a resolution of 5 mm and 60 s (the resolution of available cable temperatures). The experiment setup is shown in Figure 1. The temperature measured in the lower cable provided the lower boundary condition. The surface temperature, the upper boundary condition, was measured in the cable from the DTS unit to where it entered the ground. For a window of 24 h, the MATLAB function fminsearch was used to find the diffusivity value that minimized the root-mean-square error between the simulated and observed temperature at the depth of the upper cable. Fminsearch is a multidimensional unconstrained nonlinear minimization algorithm that uses the Nelder-Mead direct search method. For the first time step, linear interpolation between the three temperature measurements was used to give the initial temperature profile.

[16] A single estimated thermal diffusivity is obtained for the full ~10 cm using this approach, so it is assumed that thermal diffusivity is homogeneous over this depth. The derived soil moisture is therefore an integrated measure of soil moisture in the top 10 cm. Furthermore, as discussed by *Bristow* [2002], the diffusivity estimated here is really an "apparent" diffusivity because it assumes that conduction is the only mechanism of heat transfer. This apparent diffusivity is influenced by sensible and latent convective heat transfer processes which are not represented in the model, while the true diffusivity really refers to thermal conduction alone.

[17] The optimization algorithm "failed" if it did not find a diffusivity value within prescribed limits (1×10^{-8} m^2 s^{-1}, 1×10^{-5} m^2 s^{-1}). These conservative limits are well beyond the physical range expected from the models discussed in section 2.2. In the event of failure, linear interpolation between the three temperature measurements was used to reinitialize the model.

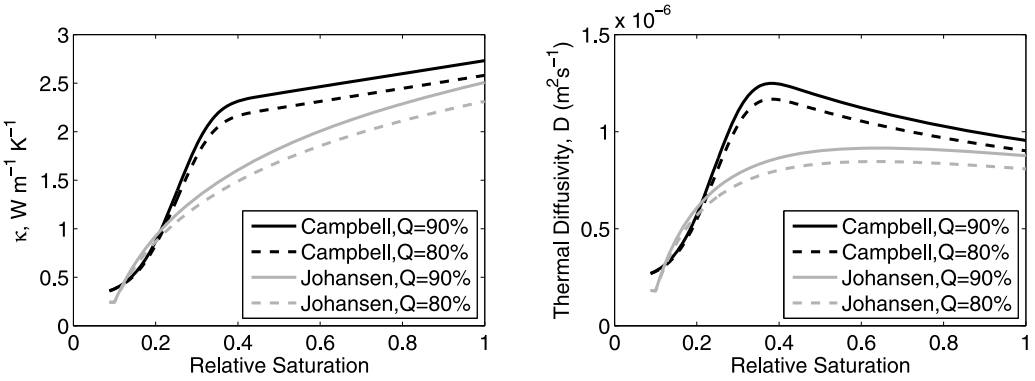

Figure 2. Thermal (left) conductivity and (right) diffusivity as functions of relative saturation calculated using the models of *Johansen* [1975] and *Campbell* [1985] assuming two different values for quartz content Q.

[18] A "moving window" was used to resolve changes in soil moisture at finer than daily resolution; the 24 h optimization window was shifted in 3-hourly increments. In section 4, the diffusivity at each 3-hourly time step is that which gives the best fit in the subsequent 24 h period. The initial condition was given by the best estimate for that time step from the previous window's estimation result. Because of sensitivity of the solution to depth and the known variable depth of the cables (Figure 1), each 2 m segment of cable was modeled separately.

2.2. Soil Moisture From Soil Thermal Properties

[19] The volumetric heat capacity of soil (J m^{-3} K^{-1}) is a simple, well-understood linear function of soil moisture:

$$C = \rho_m c_m = \frac{V_a}{V_t}\rho_a c_a + \frac{V_w}{V_t}\rho_w c_w + \frac{V_s}{V_t}\rho_s c_s$$
$$C = n(1 - S_r)\rho_a c_a + S_r n \rho_w c_w + (1 - n)\rho_s c_s, \quad (2)$$

where the subscripts m, a, t, w, and s denote the bulk soil, air, total, water, and soil solids, respectively; ρ is the density in kg m^{-3}; V represents volume; c is the specific heat capacity; S_r is the relative saturation; and n is the porosity.

[20] Thermal conductivity is considerably more complicated. In dry soil, thermal conductivity is dominated by the contribution of the air fraction, so there is little variability in dry thermal conductivity among different soils. As the soil becomes wetter, a thickening water film increases connectivity between soil particles, causing a sharp increase in thermal conductivity. As the soil approaches saturation, the thermal properties of the solids fraction dominate and because the particles are already well connected, the rate at which thermal conductivity increases is reduced.

[21] Of the many models available, those of *Johansen* [1975] and *Campbell* [1985] are used here to illustrate the challenges of obtaining soil moisture given the thermal diffusivity or conductivity. *Johansen* [1975] calculates the thermal conductivity as a linear combination of the dry and saturated thermal conductivities using a Kersten coefficient [*Kersten*, 1949] which depends on relative saturation and whether the soil is considered coarse or fine. Calculation of the dry and saturated conductivities requires the bulk density, porosity, and quartz content of the soil. *Campbell* [1985] uses an empirical equation derived from the laboratory-based thermal conductivity measurements of *McInnes* [1981]. Thermal conductivity is expressed as a function of volumetric soil moisture and five coefficients that depend on the volume fractions of soil solids, quartz, and other minerals as well as the bulk density and the clay mass fraction of the soil.

[22] Figure 2 presents the thermal conductivity and thermal diffusivity calculated using the *Johansen* [1975] and *Campbell* [1985] models for a loamy sand. Because of the high thermal conductivity of quartz (7.7 W m^{-1} K^{-1}) compared to that of other minerals (2.0–3.0 W m^{-1} K^{-1}), both models are sensitive to the quartz fraction. Figure 2 shows the calculated thermal properties for quartz fractions of 80% and 90%, highlighting the need to determine the quartz content accurately. Thermal diffusivity from the Johansen and Campbell models is a monotonic function of relative saturation up to $D = 8.7579 \times 10^{-7}$ m^2 s^{-1} and $D = 9.4809 \times 10^{-7}$ m^2 s^{-1}, respectively. Without additional information, it is impossible to infer a unique relative saturation from a thermal diffusivity value above these threshold values. It is clear from Figure 2 that the choice of thermal conductivity model will influence the final soil moisture from the estimated thermal diffusivity.

3. Experiment Design

[23] This feasibility study was conducted from June to October 2008 on the grounds of the drinking water pumping station in Monster (52°07′N, 4°17′E), Netherlands. This secure site ensured minimal disturbance to the equipment. The site had a calcaire Regosol [*European Commission Joint Research Centre*, 2005], with a loamy sand texture and sparse grass cover. The results presented in this paper are based on DTS data collected from 11 September to 9 October 2008, during which contemporaneous validation and meteorological data were available.

[24] A Halo-DTS system from Sensornet was used in this experiment. This system is suitable for use with cables up to 4 km long, can detect temperature changes of 0.1 K at a measurement integration time of 10 s, and has a spatial resolution of 2 m. Here measurements were taken with an integration time of 60 s, improving the accuracy further. Armored two-fiber multimode 50/125 μm optic cable from Kaiphone Technology was laid in a loop, as shown in Figure 1, to observe temperatures at two depths. The dis-

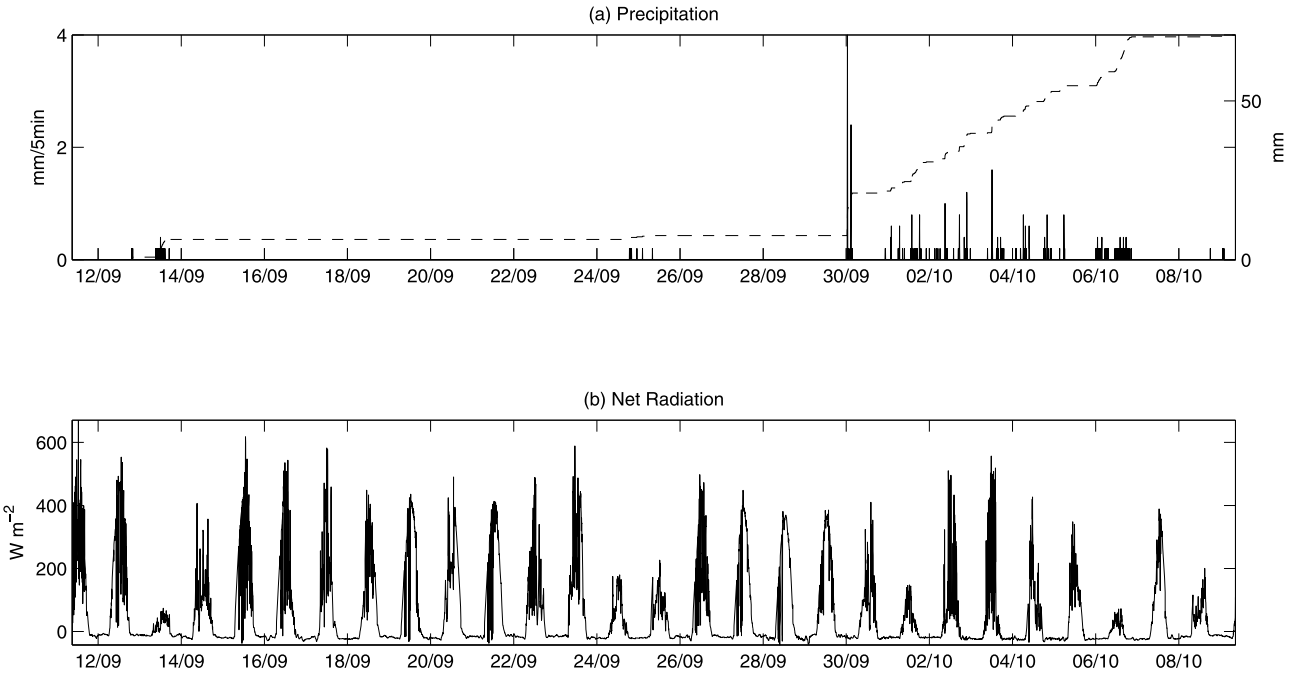

Figure 3. Precipitation and net radiation at Monster, Netherlands, from 11 September to 9 October 2008. Precipitation was measured in 5 min intervals (bars, left axis), and the cumulative precipitation is also shown (dotted line, right axis). Net radiation was calculated using measured shortwave radiation, temperature, and relative humidity, as discussed in section 2.

turbance due to the plowing of the cable was negligible because of the unstructured and loosely packed loamy sand at the site. Prior to the removal of the cable at the end of the experiment, trenches were dug along the length of the cable, and the cable depths were measured using a laser level. Figure 1 shows that the depth of cable installation increased with distance from the DTS unit. The mean depths of the upper and lower cables were 7.85 and 9.98 cm, with standard deviations of 1.35 and 1.31 cm and ranges of 4.9 and 4.7 cm, respectively. The mean distance between the upper and lower cables was 2.13 cm, with a standard deviation of 0.55 cm. It is important to note that the surface temperature observations were not colocated with those at depth. The surface temperatures used here were measured in the PVC tube containing the cable, between the DTS unit and the location where the cable enters the ground. In this study, because the study area is small and has uniform soil, cover, and meteorological conditions, it is reasonable to assume that surface temperature is almost uniform in space.

[25] A HOBO® weather station (Onset Computer Corporation, http://www.onsetcomp.com/products/weather_stations) measured pressure, air temperature, relative humidity, downward shortwave radiation, precipitation, wind direction, and wind speed. These data were combined with the surface cable temperature to calculate net radiation. Downward longwave radiation (LW_{down}) from the atmosphere was calculated using equations (3) and (4) [*Bras*, 1990]:

$$LW_{down} = \sigma E_a T_a^4, \tag{3}$$

where σ is the Stefan-Boltzmann constant and T_a is the air temperature in Kelvin. E_a is the atmospheric emissivity given by

$$E_a = 0.74 + 0.0049e, \tag{4}$$

where e is the vapor pressure in millibars. Upward longwave radiation (LW_{up}) from the surface was given by

$$LW_{up} = \sigma E_s T_s^4, \tag{5}$$

where E_s is the surface emissivity, assumed to be 0.84 [*Arya*, 2001, Table 3.1], and T_s is the surface temperature in Kelvin. An albedo of 0.18 was assumed to calculate the upward shortwave radiation [*Bras*, 1990, Table 2.5]. Hourly relative saturation of the soil was measured using four ECH_2O® probes, distributed evenly (every ~9 m) along the length of the cable as illustrated in Figure 1.

4. Results

4.1. Meteorological Observations

[26] Meteorological data are not required in any of the calculations discussed here. However, precipitation and net radiation data are shown in Figure 3 to identify when changes in soil moisture are expected to be seen.

[27] A total of 71 mm of precipitation was recorded during this period, most of which occurred between 30 September and 6 October following a fortnight of dry weather. The highest daily amounts (14.0 and 15.5 mm, respectively) occurred on these two dates.

[28] Net radiation was considerably reduced on 13, 24, and 25 September as well as 1 and 6 October 2008. In section 4.4, it will be shown that this poses a challenge to retrieving soil moisture using the technique discussed here.

4.2. Relative Saturation Observed With ECH_2O Probes

[29] Relative saturation was measured using four ECH_2O EC-10 probes from Decagon Devices (user's manual available at http://www.decagon.com/pdfs/manuals/EC-20_EC-

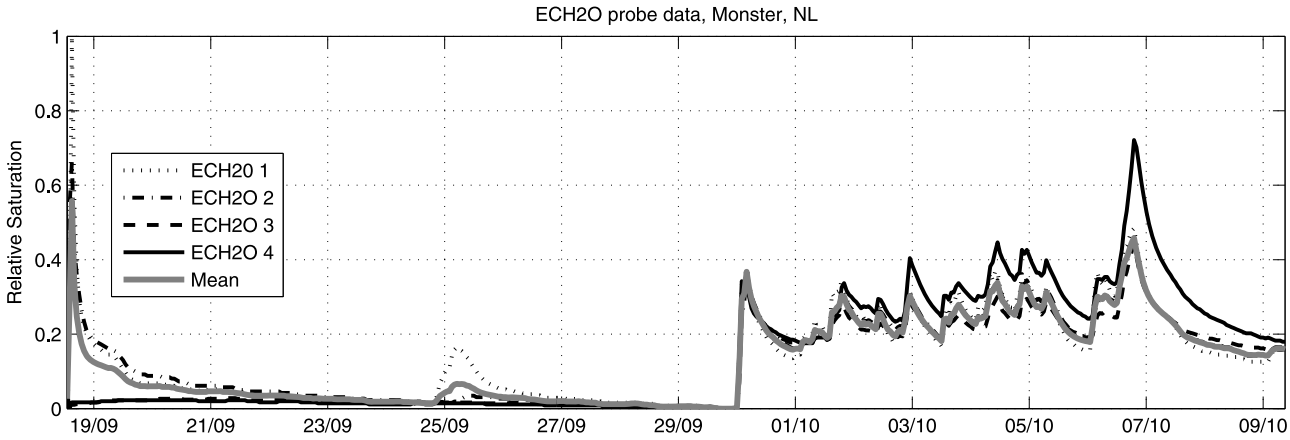

Figure 4. Relative saturation observed using ECH_2O probes from 18 September to 9 October 2008 at the Monster study site. The mean is shown in grey.

10_EC-5_v8.pdf). The sensors were inserted vertically and thus measured relative saturation in the top 14.5 cm. Calibrated observations from the four probes are shown in Figure 4. An artificial rainfall experiment was conducted on 18 September 2008 in the vicinity of ECH_2O 1. Elevated relative saturation was also observed at ECH_2O 2, but the remaining probes were unaffected. By 29 September, the soil was completely dry. Both completely wet and dry conditions

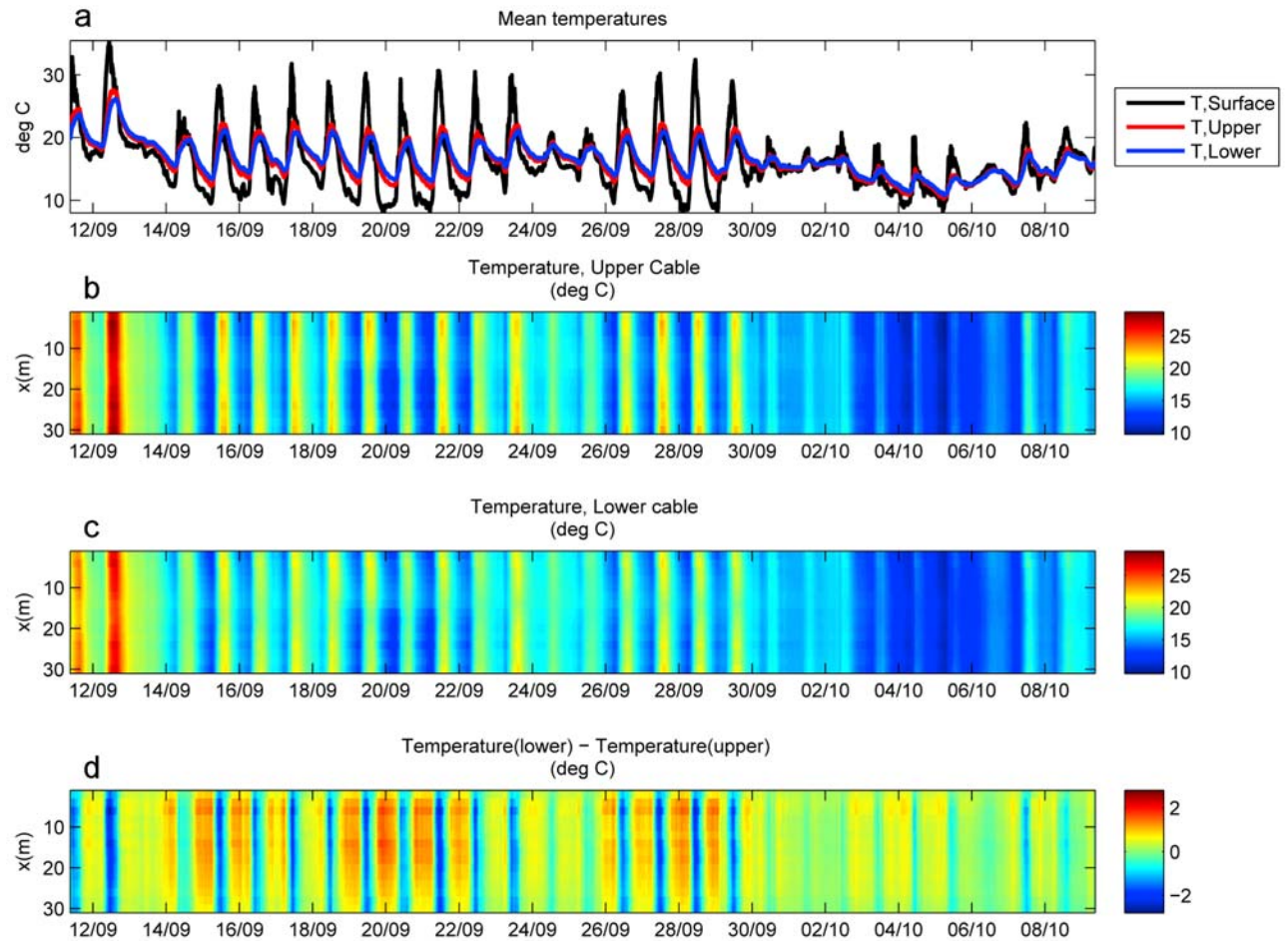

Figure 5. Temperatures recorded in the cables at the surface and in the upper and lower levels (mean depths of 7.85 and 9.98 cm, respectively), showing (a) the spatially averaged temperature at each depth as a function of time, the spatial distribution of temperature in the (b) upper and (c) lower cables, and (d) the spatial distribution of the difference between the temperature at the lower cable and the upper cable.

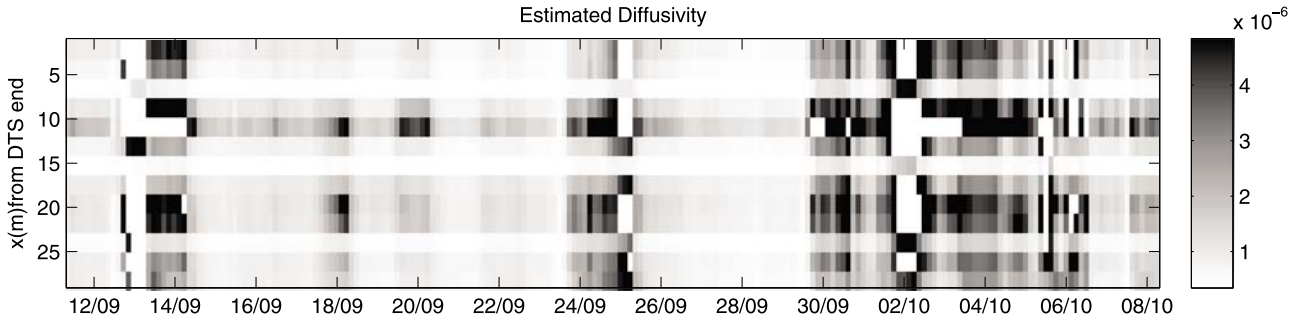

Figure 6. Thermal diffusivity ($m^2\ s^{-1}$) estimated using the technique discussed in section 2.1. Distance from where the cable enters the ground at the DTS end (x in meters) is on the y axis.

were observed with ECH_2O 1, so it was used to scale the data from the other probes by assuming that the precipitation on 30 September raised the relative saturation to the same value at all probes. This assumption is valid because of the small study area and uniform soil and cover. Sharp increases are apparent following the significant events on 30 September and 6 October, while frequent smaller events maintained a relative saturation of about 0.3 between these events.

4.3. Soil Temperatures Observed With DTS

[30] Figure 5 shows the cable temperatures observed using the DTS system. As required for the successful application of this method, the cable temperatures exhibit a clear diurnal cycle in response to the diurnal variation in net radiation that is damped and attenuated with depth. At a given time, the range in temperature along both the upper and lower cables varies from 0.1°C to 2.7°C. Maximum variability occurs at the daily maximum and minimum temperatures. In general, the range is largest on clear days when downward shortwave radiation and, consequently, net radiation are highest. This spatial variability in temperature may be due to variability in soil texture or soil moisture or, more likely, to the variation in cable depth seen in Figure 1.

[31] Figure 5 also shows that temperature difference between the upper and lower cables clearly varies in time and space. During the night, the lower cable cools more slowly than the upper cable, while in the late morning to early afternoon the surface is warming and the upper cable heats up more quickly. The magnitude of the difference observed between the cables depends on the strength of the diurnal cycle in temperature, which is determined by the net radiation (Figure 3). The temperature difference between the cables varies with depth. Close to the DTS unit, where both cables are closer to the surface, the difference between them is largest.

4.4. Estimated Thermal Diffusivity

[32] Figure 6 shows the estimated thermal diffusivity as a function of distance along the cable and time. Elevated diffusivities were estimated on 13 and 24–25 September and in the week following 29 September. These were all periods in which precipitation occurred (Figure 3) and soil moisture increased (Figure 4). However, there were also many times within these intervals in which the optimization algorithm failed to converge on an optimum value. This can be attributed to the low net radiation values on these days (Figure 3). When daytime net radiation is low, temperature gradients are small. As the gradient goes to zero, the inversion becomes unstable. This will also pose a problem when this method is applied under dense vegetation cover. Furthermore, many of the estimated diffusivities lie beyond the reasonable range of values expected from both the Campbell and Johansen models. The maximum expected value is on the order of $1.25 \times 10^{-6}\ m^2\ s^{-1}$ (Figure 2). The horizontal striping in Figure 6 shows that the estimated diffusivity varied with location along the length of the cable. The three horizontal bands apparent at $x = 6$ m, $x = 14$ m, and $x = 22$ m are the cable segments in which the estimated diffusivities generally fall within the physically plausible range.

[33] Figure 7 examines the potential role of the distance between the cables in obtaining a reasonable estimate for thermal diffusivity. Time series of estimated diffusivities from four 2 m cable segments are shown. The two diffusivities in black are from $x = 6$ m and $x = 14$ m, where the distance between the cables was 3 and 2.95 cm, respectively. In both cases, the estimated diffusivity is typically within the plausible range. A single data gap, which can be attributed to low net radiation, occurs on 5 October. The estimated diffusivities at $x = 8$ m and $x = 20$ m are shown in grey. Here the cables were just 1.6 and 1.5 cm apart. The

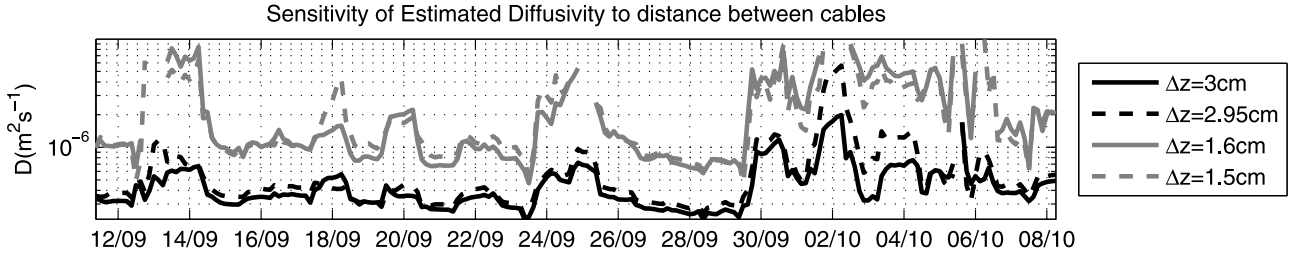

Figure 7. Estimated thermal diffusivity at selected locations along the cable. The cable segments shown were at $x = 14$, $x = 6$, $x = 8$, and $x = 20$ m, respectively.

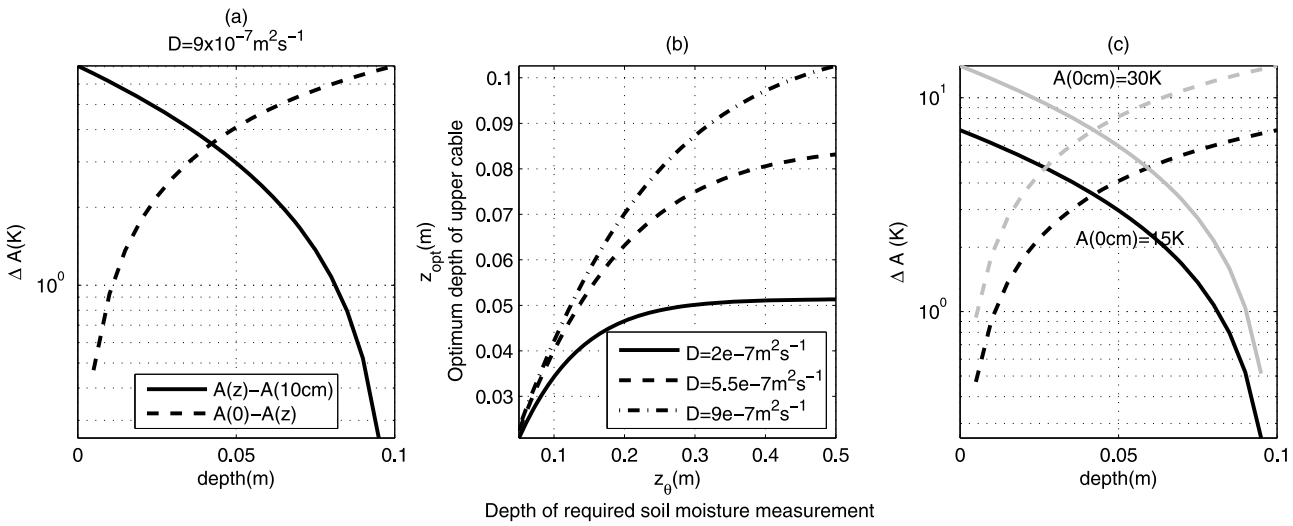

Figure 8. Calculating the optimum cable depth to estimate soil moisture between the surface and depth z_θ (in meters). For A_s = 15 K and $D = 2.5 \times 10^{-7}$ m^2 s^{-1}, (a) the difference in amplitude between a cable at depth z and the cables at the surface and lower boundary where z_θ = 0.1 m is shown. (b) The optimum cable depth (z_{opt}) and (c) the difference in amplitude between a cable at z_{opt} and the boundaries are also shown.

same temporal pattern is apparent, with increased diffusivity estimated in periods of elevated soil moisture. However, the estimated diffusivities are almost always higher than the reasonable range. There are also more cases when the optimization algorithm failed to converge on a solution. This suggests that the cables must be some minimum distance apart to reliably estimate the thermal diffusivity. To investigate this further, the diffusion model was used to simulate the response at depth to a sinusoidal surface temperature pattern.

4.4.1. Hypothetical Cable Depth for Optimum Performance of Inversion Approach

[34] The analysis is in terms of amplitude, which varies only with depth, rather than temperature, which varies with both time and depth. For a sinusoidal surface temperature with amplitude A_s and period P, the amplitude at some soil depth z is given by

$$A(z) = A_s \exp\left(-z\sqrt{\frac{\pi}{PD}}\right), \tag{6}$$

where D is the thermal diffusivity of the soil [e.g., *Arya*, 2001]. To determine soil moisture from the surface to depth z_θ, cables are placed at the surface (z = 0 cm) and at the lower boundary ($z = z_\theta$). The inversion method requires a third cable somewhere between these two. Figure 8a shows the temperature amplitude difference between a hypothetical cable at depth z and one both at the surface (dashed line) and at 10 cm depth (solid line). The optimum depth for this hypothetical cable, z_{opt}, is where these amplitude differences are equal. This occurs where the amplitude is the mean of the amplitudes in the surface and lower cables:

$$A(z_{\text{opt}}) = \frac{A_s + A(z_\theta)}{2}. \tag{7}$$

Substituting the values for the amplitude at z_θ and z_{opt} and rearranging yields the following expression for the optimum cable depth:

$$z_{\text{opt}} = -\sqrt{\frac{PD}{\pi}}\log\left\{\frac{1}{2}\left[\exp\left(-z_\theta\sqrt{\frac{\pi}{PD}}\right)+1\right]\right\}. \tag{8}$$

This optimum depth is at the intersection of the two curves in Figure 8a. Note that the optimum depth depends only on the soil thermal diffusivity and the depth z_θ. The difference in amplitude between either boundary and z_{opt}, on the other hand, is proportional to the surface amplitude:

$$\Delta A(z_{\text{opt}}) = A_s - A(z_{\text{opt}}) = \frac{A_s}{2}\left[1 - \exp\left(-z_\theta\sqrt{\frac{\pi}{PD}}\right)\right]. \tag{9}$$

Higher values of ΔA imply that changes in temperature and therefore diffusivity are more readily detectible. Its dependence on A_s explains why reduced net radiation (which reduces A_s) limits our ability to estimate diffusivity and soil moisture from temperature observations. From Figures 8b and 8c, using the lowest value of diffusivity for a given soil yields the most conservative estimate of z_{opt}, i.e., closest to the surface with the highest value of ΔA. The thermal diffusivity of dry soil should therefore be used to determine the optimum cable depth. Recall from section 2.2 that there is little variability in this quantity among soil types, so the optimum depth will vary little by soil type.

[35] Assuming $D = 2 \times 10^{-7}$ m^2 s^{-1}, Figure 8a shows that the optimal cable depth to measure soil moisture from 0 to 0.10 m is 0.034 m and that ΔA at this depth is 5.6 K for A_s = 15 K. Placing the cable at 0.07 or 0.085 m reduces the corresponding values of ΔA to just 1.9 or 0.9 K, respectively. This explains why the diffusivity estimate appears to improve with increasing distance between the lower cables in Figure 7. Placing the cable closer to the optimal depth

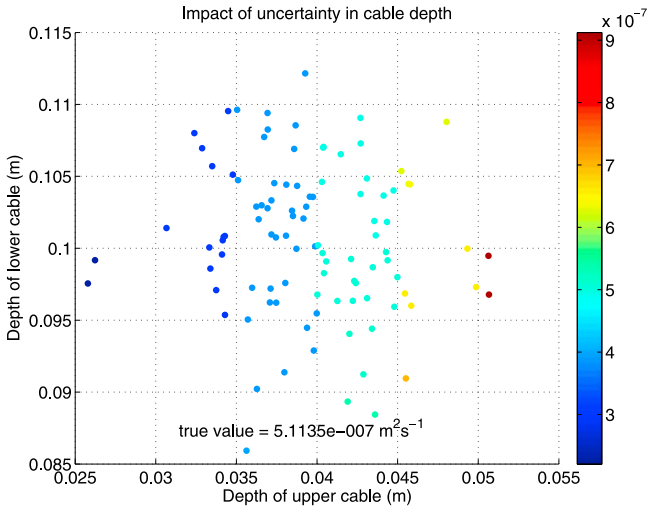

Figure 9. The impact of uncertainty in the cable depths on the temporal mean of the estimated diffusivity. The color of each dot indicates the value of the estimated diffusivity. The true value refers to the diffusivity value calculated from the observed relative saturation and was used to simulate the temperatures at 4 and 10 cm.

leads to more reliable estimates of diffusivity and hence soil moisture.

4.4.2. Impact of Uncertainty in Cable Depth

[36] A Monte Carlo experiment, with 100 ensemble members, was conducted to demonstrate the impact that uncertainty in the cable depth has on the estimated diffusivity. The Johansen model (assuming 90% quartz content) was used to generate a time series of thermal diffusivity values from the relative saturation values plotted in Figure 4. Assuming these values for diffusivity in the heat diffusion model (equation (1)) and forcing the surface boundary with the temperature data from the surface cable, a time series of temperature at 4 cm depth was simulated. This depth was chosen as it is close to the optimal hypothetical depth from section 4.4.1. The inversion approach was used to estimate the diffusivity, but assuming that the depths of the upper and lower cables were uncertain, each with an error standard deviation of 0.5 cm.

[37] Figure 9 shows the mean diffusivity estimated for each pair of uncertain cable depths. The mean value of the true diffusivity was 5.1×10^{-7} m^2 s^{-1}. The impact of uncertainty in the depth of the upper cable is much more significant than in the lower cable because the temperature fluctuations at depth are smaller, so there is less difference between model layers. An error with a standard deviation of 0.5 cm in a cable at 4 cm depth leads to diffusivity estimates spanning the full dynamic range. If the upper cable depth is assumed to be shallower than the true depth, the diffusivity is underestimated.

[38] Figure 10 shows the time series of estimated diffusivity for each assumed cable depth pair, with the true diffusivity shown in black. The apparent grouping of diffusivity estimates is due to the discretization of the diffusion model ($dz = 0.005$ m). Figure 10 shows that the impact of uncertainty in cable depth is most significant at high values of diffusivity. At very high values of diffusivity, assuming the incorrect cable depth can lead to physically implausible (high) values of thermal diffusivity. This underscores the importance of correctly determining the cable depths. The overestimation of thermal diffusivity in Figure 7 could be because the cable depth was overestimated.

4.5. Estimated Soil Moisture

[39] Figure 11 shows the soil moisture inferred from the estimated diffusivities for two 2 m segments, those at 6 and 14 m from the DTS unit. These segments are shown in Figure 7 to give the most reasonable estimated diffusivity values.

[40] For most of the experiment up to 29 September the estimated diffusivity was very low. Consequently, both the Johansen and Campbell models yield unique and comparable estimates for relative saturation. While Figure 4 suggests that the soil was completely dry by 29 September, it is important to note that both thermal conductivity models are only defined above relative saturation of 0.1. In dry soils, a small change in relative saturation leads to a large increase in thermal diffusivities, so, despite the variability in Figure 7 during this dry period, the estimated relative saturation is nearly constant.

[41] Figure 7 shows that elevated diffusivities were detected for these segments during the week of 29 September to 6 October, consistent with the increased soil moisture shown in Figure 4. However, these diffusivities were higher than the maximum expected from both the Johansen and Campbell models for this loamy sand. Consequently, there are many gaps in estimated soil moisture during this wet period. There are three possible causes of this problem:

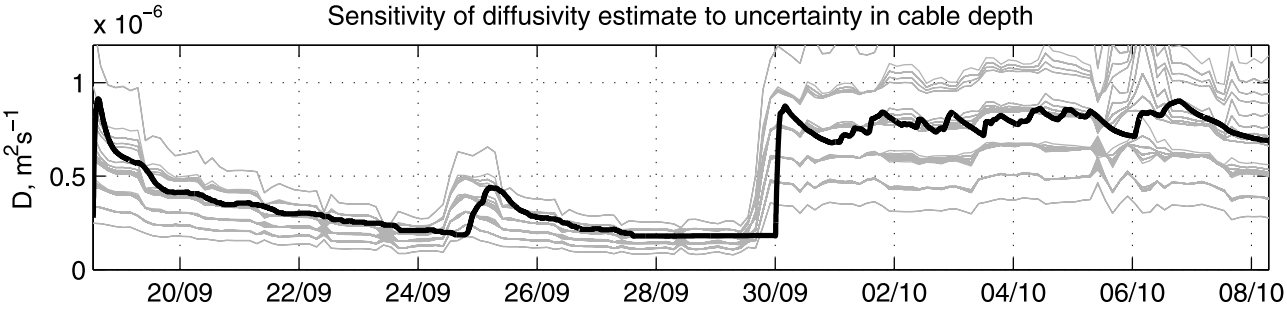

Figure 10. Sensitivity of diffusivity estimate to uncertainty in the cable depth. Each grey line is the diffusivity estimate from an assumed pair of cable depths. The true (simulated) diffusivity is superimposed in black.

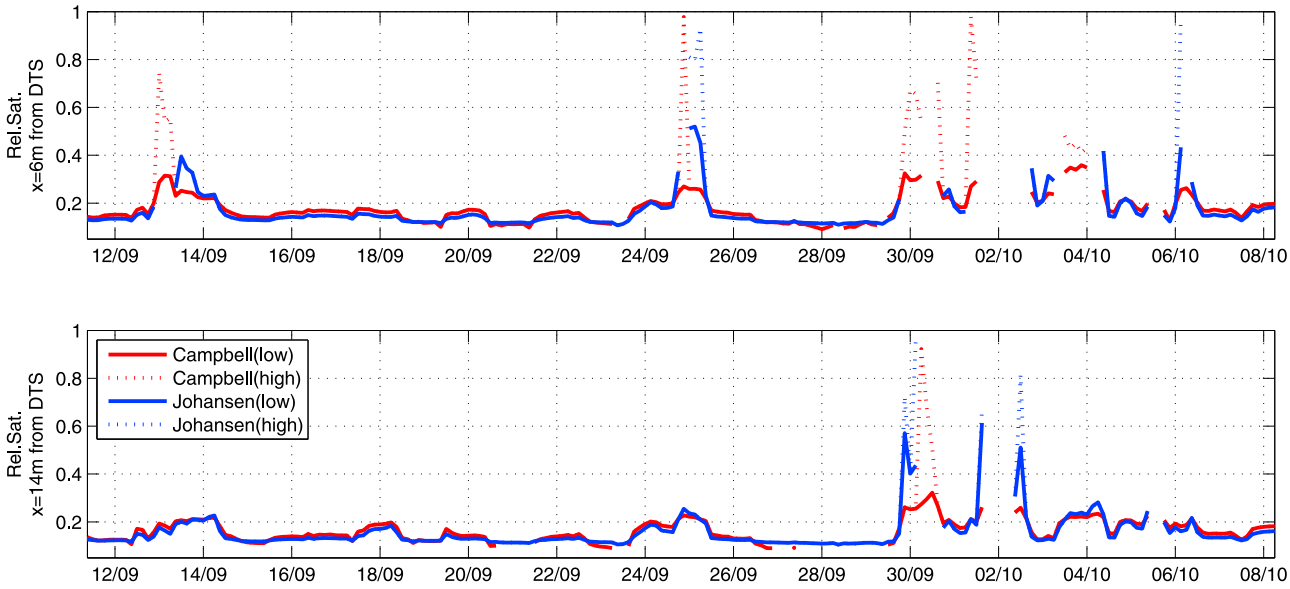

Figure 11. Inferred relative saturation from the estimated thermal diffusivities at (top) x = 6 m and (bottom) x = 14 m using the *Campbell* [1985] and *Johansen* [1975] models. Above a diffusivity threshold in each of the models, relative saturation is a nonunique function of thermal diffusivity. "Low" and "high" assume the relative saturation value less than and greater than that associated with the maximum thermal diffusivity.

(1) neither the Johansen nor the Campbell model correctly describes the relationship between relative saturation and thermal diffusivity for this soil; (2) the distance between the cables is still too small (section 4.4.1) and/or the cable depth is incorrect (section 4.4.2); and (3) the diffusion model was invalid during this period because of heat advection as water infiltrated the unsaturated zone.

[42] Another interesting feature of Figure 11 is attributable to the nature of the relationship between thermal conductivity and relative saturation, that above some value the increase in thermal conductivity with relative saturation slows down. Above this critical value, it is impossible to infer a unique relative saturation value for a given thermal conductivity or diffusivity. For each model, both possible solutions are shown in Figure 11. The threshold in the Campbell model is higher than the maximum value from the Johansen model, so in some cases (e.g., for x = 6 m on 25 September), the Campbell model will give two possible values (one greater than and one less than the maximum), while the Johansen model gives none. If the diffusivity is between the threshold value from Johansen and that from Campbell, the Campbell model gives a unique estimate for the relative saturation, while the Johansen model yields two possible values (e.g., after initial increase on 29 September, for x = 14 m). Clearly, the inability to distinguish between relative saturation of ~0.2 and ~1.0 is unacceptable. This indicates that some prior knowledge of soil moisture would add value to this estimate. In section 5, details on how to address this serious shortcoming will be presented.

5. Conclusions and Discussion

[43] A feasibility study was conducted to investigate the possibility of using passive soil DTS to observe soil moisture. Cables were installed at two depths to monitor temperature changes in response to net radiation. The hypothesis was that the cable temperatures could be used to estimate soil thermal properties from which soil moisture could be inferred.

[44] *Béhaegel et al.* [2007] estimated 15 day soil moisture in the thermally active layer by simulating heat diffusion and finding the thermal diffusivity which gave the best agreement with observed temperature at 60 cm. Here a similar inversion approach was used to estimate soil moisture in the top 10 cm of soil, where the boundary conditions and temperature to be matched were all measured using passive soil DTS. Soil moisture was estimated in 24 h moving windows shifted in 3-hourly increments. While it was shown that changes in soil moisture resulted in detectable changes in thermal diffusivity, the shorter estimation or optimization window posed several problems.

[45] 1. In a longer time window, it seems a more reasonable assumption that diffusion is the dominant heat transfer process because the duration of a precipitation event is a smaller fraction of the study interval.

[46] 2. The temperatures vary primarily in response to the diurnal variability in net radiation. If net radiation is low for a given day, there is very little temperature response to measure. In a 15 day estimation window (e.g., as used by *Béhaegel et al.* [2007]) this is less problematic unless net radiation is low for the entire 15 day window.

[47] 3. A longer study interval implies an effective diffusivity for a longer period, so the results are effectively averaged. This reduces the likelihood of obtaining extreme values beyond the physically reasonable range.

[48] The usefulness of inverse methods is further limited by the nature of the relationship between thermal diffusivity and relative saturation. At low relative saturation, a minute change in relative saturation leads to a dramatic increase in diffusivity, while diffusivity is largely insensitive to changes at higher relative saturation. Furthermore, it is impossible to

infer a single relative saturation from a diffusivity value for at least half of the dynamic range.

[49] While this study demonstrated that passive soil DTS could indeed detect changes in soil moisture, it also highlighted several reasons why data assimilation might be a more appropriate method of estimating soil moisture than conventional inverse methods. In a data assimilation approach, the cable temperatures can be used to constrain a coupled heat-moisture transport model. Future research will focus on a dual state-parameter estimation approach [e.g., *Moradkhani et al.*, 2005], in which temperature will be estimated as a state and soil moisture will be estimated as a parameter of the model. Thermal properties are calculated from soil moisture in forward simulations, avoiding the nonuniqueness problem in the other direction. The model can be adapted to include advection, evaporation, or any additional processes considered significant. Accounting for these processes ensures that the true, rather than the "apparent," thermal diffusivity is estimated. Soil temperature and moisture content can be estimated at all depths in the desired profile at the resolution of the coupled model, yielding a profile of surface and root zone soil moisture rather than a single integrated measure between the cables.

[50] Even using data assimilation techniques, many of the technical challenges remain. Several lessons from this study will be used to address these more practical issues. First, the cable depths must be well known and the cables must be sufficiently far apart for there to be a measurable difference in temperature. The plow design and installation method will be revised to ensure that cables are installed a fixed and known distance apart. The cable depth can be determined by amplitude analysis for a given soil moisture if the relationship between thermal diffusivity and soil moisture is known using probe measurements [e.g., *Mori et al.*, 2003]. A method was presented to calculate the optimum cable depth to measure soil moisture over a prescribed depth. To measure soil moisture from 0 to 10 cm, for example, cables are required at 0, 10, and 3.4 cm. In this experiment in a fine sand Regosol with weak to absent soil structure, there was little disturbance due to the plowing of the cable. However, if cables are plowed into soils containing fine sediments or clay, a recovery period would be required before the first useful observations to ensure that the measurements could be considered representative of the surrounding undisturbed soil.

[51] In this experiment, a single series of surface temperature was available. Because the experiment was conducted in a very small area with uniform soil, cover, and meteorological conditions, it is reasonable to assume that surface temperature is homogeneous. However, to account for spatial variability, future larger-scale experiments will have a colocated cable to measure surface temperature.

[52] Finally, the relationship between thermal conductivity and soil moisture is critical. This must be ascertained through in situ measurements over the full dynamic range of saturation values. This is the key link between soil moisture and soil temperature, and its significance cannot be underestimated if passive soil DTS is to be developed into a viable approach to measure large-scale variability in soil moisture.

[53] **Acknowledgments.** Partial support for M.H. and S.W.T. was provided from U.S. Bureau of Reclamation agreement 06FC204044. The authors are grateful to three anonymous reviewers, the Associate Editor, and the Editor, whose comments and suggestions improved the quality of the manuscript.

References

Anthes, R., et al. (2007), *Earth Science and Applications from Space: National Imperative for the Next Decade and Beyond*, Natl. Acad. Press, Washington, D. C.

Arya, S. P. (2001), *Introduction to Micrometeorology*, *Int. Geophys. Ser.*, vol. 79, 2nd ed., 420 pp., Academic, San Diego, Calif.

Béhaegel, M., P. Sailhac, and G. Marquis (2007), On the use of surface and ground temperature data to recover soil water content information, *J. Appl. Geophys.*, *62*(3), 234–243, doi:10.1016/j.jappgeo.2006.11.005.

Bras, R. L. (1990), *Hydrology: An Introduction to Hydrologic Science*, Addison-Wesley, Reading, Mass.

Bristow, K. L. (2002), Soil heat, in *Methods of Soil Analysis. Part 4, Physical Methods*, edited by J. H. Dane and G. C. Topp, pp. 1183–1248, Soil Sci. Soc. of Am., Madison, Wis.

Campbell, G. S. (1985), *Soil Physics with BASIC: Transport Models for Soil-Plant Systems*, 3rd ed., 150 pp., Elsevier, New York.

Campbell, G. S., C. Calissendorff, and J. H. Williams (1991), Probe for measuring soil specific heat using a heat-pulse method, *Soil Sci. Soc. Am. J.*, *55*, 291–293.

Cosh, M. H., T. J. Jackson, R. Bindlish, and J. H. Preuger (2004), Watershed scale temporal and spatial variability of soil moisture and its role in validating soil moisture estimates, *Remote Sens. Environ.*, *92*, 427–435, doi:10.1016/j.rse.2004.02.016.

Entekhabi, D., I. Rodriguez-Iturbe, and F. Castelli (1996), Mutual interaction of soil moisture state and atmospheric processes, *J. Hydrol.*, *184*, 3–17, doi:10.1016/0022-1694(95)02965-6.

European Commission Joint Research Centre (2005), *Soil Atlas of Europe*, 128 pp., Eur. Communities, Luxembourg.

Gurney, R. J., and P. J. Camillo (1984), Modelling daily evapotranspiration using remotely sensed data, *J. Hydrol.*, *69*, 305–324, doi:10.1016/0022-1694(84)90170-7.

Idso, S. B., T. J. Schmugge, R. D. Jackson, and R. J. Reginato (1975a), The utility of surface temperature measurements for the remote sensing of surface soil water status, *J. Geophys. Res.*, *80*, 3044–3049, doi:10.1029/JC080i021p03044.

Idso, S. B., R. D. Jackson, and R. J. Reginato (1975b), Detection of soil moisture by remote surveillance, *Am. Sci.*, *63*, 549–557.

Idso, S. B., R. D. Jackson, and R. J. Reginato (1976), Compensating for environmental variability in the thermal inertia approach to remote sensing of soil moisture, *J. Appl. Meteorol.*, *15*, 811–817, doi:10.1175/1520-0450(1976)015<0811:CFEVIT>2.0.CO;2.

Jacobs, J. M., B. P. Mohanty, E.-C. Hsu, and D. Miller (2004), SMEX02: Field scale variability, time stability and similarity of soil moisture, *Remote Sens. Environ.*, *92*, 436–446, doi:10.1016/j.rse.2004.02.017.

Johansen, O. (1975), Thermal conductivity of soils, Ph.D. thesis, 236 pp., Univ. of Trondheim, Trondheim, Norway.

Kamai, T., A. Tuli, G. J. Kluitenberg, and J. W. Hopmans (2008), Soil water flux density measurements near 1 cm d^{-1} using an improved heat pulse probe design, *Water Resour. Res.*, *44*, W00D14, doi:10.1029/2008WR007036.

Kerr, Y. H., P. Waldteufel, J.-P. Wigneron, J. Martinuzzi, J. Font, and M. Berger (2001), Soil moisture retrieval from space: The Soil Moisture and Ocean Salinity (SMOS) mission, *IEEE Trans. Geosci. Remote Sens.*, *39*(8), 1729–1735, doi:10.1109/36.942551.

Kersten, M. S. (1949), *Thermal Properties of Soils*, *Minn. Univ. Eng. Exp. Stn. Bull.*, *52*, 227 pp.

Kluitenberg, G. J., K. L. Bristow, and B. S. Das (1995), Error analysis of heat pulse method for measuring soil heat capacity, diffusivity, and conductivity, *Soil Sci. Soc. Am. J.*, *59*, 719–726.

Liu, G., B. Li, T. Ren, R. Horton, and B. C. Si (2008), Analytical solution of heat pulse method in a parallelepiped sample space with inclined needles, *Soil Sci. Soc. Am. J.*, *72*, 1208–1216, doi:10.2136/sssaj2007.0260.

McInnes, K. J. (1981), Thermal conductivities of soils from dryland wheat regions of eastern Washington, M.S. thesis, 51 pp., Wash. State Univ., Pullman.

Mohanty, B. P., and T. H. Skaggs (2001), Spatio-temporal evolution and time-stable characteristics of soil moisture within remote sensing footprints with varying soil, slope, and vegetation, *Adv. Water Resour.*, *24*, 1051–1067, doi:10.1016/S0309-1708(01)00034-3.

Moradkhani, H., S. Sorooshian, H. V. Gupta, and P. R. Houser (2005), Dual state-parameter estimation of hydrological models using ensem-

ble Kalman filter, *Adv. Water Resour.*, *28*, 135–147, doi:10.1016/j.advwatres.2004.09.002.

Mori, Y., J. W. Hopmans, A. P. Mortensen, and G. J. Kluitenberg (2003), Multi-functional heat pulse probe for the simultaneous measurement of soil water content, solute concentration, and heat transport parameters, *Vadose Zone J.*, *2*, 561–571, doi:10.2113/2.4.561.

Mortensen, A. P., J. W. Hopmans, Y. Mori, and J. Šimůnek (2006), Multi-functional heat pulse probe measurements of coupled vadose zone flow and transport, *Adv. Water Resour.*, 29, 250–267, doi:10.1016/j.advwatres.2005.03.017.

Price, J. C. (1977), Thermal inertia mapping: A new view of the Earth, *J. Geophys. Res.*, *82*, 2582–2590, doi:10.1029/JC082i018p02582.

Rosema, A. (1975), Simulation of the thermal behavior of bare soils for remote sensing purposes, in *Heat and Mass Transfer in the Biosphere*, *Adv. Thermal Eng.*, vol. 3, edited by D. A. deVries and N. H. Afgan, pp. 109–123, Scripta, Washington, D. C.

Selker, J. S., L. Thevenaz, H. Huwald, A. Mallet, W. Luxemburg, N. van de Giesen, M. Stejskal, J. Zeman, M. Westhoff, and M. B. Parlange (2006), Distributed fiber-optic temperature sensing for hydrologic systems, *Water Resour. Res.*, *42*, W12202, doi:10.1029/2006WR005326.

Tyler, S. W., J. S. Selker, M. B. Hausner, C. E. Hatch, T. Torgersen, C. E. Thodal, and S. G. Schladow (2009), Environmental temperature sensing using Raman spectra DTS fiber-optic methods, *Water Resour. Res.*, *45*, W00D23, doi:10.1029/2008WR007052.

Vachaud, G., A. P. De Silans, P. Balabanis, and M. Vauclin (1985), Temporal stability of spatially measured soil water probability density function, *Soil Sci. Soc. Am. J.*, *49*, 822–828.

Van De Griend, A. A., P. J. Camillo, and R. J. Gurney (1985), Discrimination of soil physical parameters, thermal inertia, and soil moisture from diurnal surface temperature fluctuations, *Water Resour. Res.*, *21*(7), 997–1009, doi:10.1029/WR021i007p00997.

T. A. Bogaard, D. M. Krzeminska, M. M. Rutten, S. C. Steele-Dunne, and N. C. van de Giesen, Water Resources Section, Faculty of Civil Engineering and Geosciences, Delft University of Technology, PO Box 5048, NL-2600 GA Delft, Netherlands. (s.c.steele-dunne@tudelft.nl)

M. Hausner and S. W. Tyler, Department of Geological Sciences and Engineering, University of Nevada, Reno, Reno, NV 89557, USA.

J. Selker, Department of Biological and Ecological Engineering, Oregon State University, Corvallis, OR 97331, USA.